SURFACE FLUX – WIND PROFILE RELATIONSHIP IN CONVECTIVE CONDITIONS: A NEW RESULT

Edi Santoso[1]

Abstract

A new improved flux – profile relationship for winds in convective conditions is constructed from convective transport theory and radix layer theory. Data from the Minnesota field experiment are used to recalibrate the new parameterization and similarity equation, and data from BLX96 are used to determine whether radix layer wind profile depends on surface conditions such as roughness. The results are compared against independent data collected during the Koorin field campaign. The flux-profile relationship for wind speed is dependent on a wide-range of scales of terrain roughness. First the ML transport coefficient for momentum flux C_{*D} depends on small-scale roughness elements as affect the aerodynamic roughness length z_o. Second, shape parameter D_M depends on resolvable-scale topographic variations as affect the standard deviation of terrain elevation s_z. Such dependence over the wide range of scales should be expected because the radix layer profile equations were designed and calibrated as the average over a heterogeneous region, rather than being for one column over a single land use.

Intisari

Sebuah persamaan baru keterkaitan antara fluks dan profil untuk angin pada kondisi konvektif dibangun dari teori transpor konvektif dan teori lapisan radix. Data dari eksperimen lapangan di Minnesota digunakan untuk kalibrasi ulang. Data eksperimen lapangan BLX96 digunakan untuk menguji kebergantungan profil angin pada kondisi permukaan. Data ekperimen lapangan di Koorin digunakan untuk pembanding. Persamaan keterkaitan antara fluks dan profil untuk angin bergantung pada berbagai skala kekasaran permukaan. Pertama, koefisien transpor untuk fluks momentum bergantung pada elemen kekasaran permukaan skala kecil. Kedua, parameter bentuk profil bergantung pada variasi berskala topografi. Kebergantung pada berbagai skala seperti ini adalah konsekuensi logis dari persamaan profil di lapisan radix yang didesain dan dikalibrasi menggunakan eksperimental data yang mengakomodasi pengaruh berbagai skala.

1. INTRODUCTION

The term mixed layer (ML) is used in this paper to represent the whole convective boundary layer that is nonlocally statically unstable (Stull, 1991), and which is undergoing vigorous convective overturning associated with coherent rising thermals. Using wind speed as an example, winds are zero near the ground and smoothly increase with height until finally becoming tangent to a vertically uniform, but subgeostrophic, wind-speed layer in the mid-ML (Santoso and Stull, 1998). Across the top of the ML, the winds increase to their nearly geostrophic magnitudes above.

One can identify subdomains of the ML that have different similarity scalings. In the middle is the uniform layer (UL) as described above. Convective ML scales such as the Deardorff velocity (w_*) and ML depth (z_i) apply here, and are associated with the large thermal circulations that transport heat upward and momentum downward. The Deardorff velocity is defined as

$$w_* = \left[\left(g / T_v \right) \cdot z_i \cdot \overline{w' \theta_v'}_s \right] \qquad (1)$$

[1] UPT Hujan Buatan, BPP Teknologi, Jakarta

where g is gravitational acceleration, T_v is virtual absolute temperature, z_i is the convective boundary layer (BL) depth, $\overline{w'\theta_v'}_s$ is vertical virtual temperature flux near the surface, and subscript s denotes near-surface characteristics.

Above is the entrainment zone, a transition layer between the UL and the nearly-geostrophic free atmosphere above. Within the entrainment zone are subadiabatic temperature profiles, overshooting thermals, intermittent turbulence and wind shear (Deardorff et al., 1980). Both free convection and entrainment scales are important here (Sorbjan, 1999).

At the very bottom of the ML is the surface layer (SL), the nearly-constant flux region where Monin-Obukhov (MO) similarity theory applies (i.e., Businger et al., 1971; Dyer, 1974). In this layer the wind profile is nearly logarithmic with height (z), and is dominated by mechanically-generated small-eddy turbulence within the wall shear flow (Stull, 1997a). The dominant SL scales are aerodynamic roughness length (z_o), friction velocity (u_*), and Obukhov length (L):

$$L = -u_*^3 / \left[k \cdot \left(\frac{g}{T_v} \right) \cdot \overline{w'\theta_v'}_s \right] \qquad (2)$$

where k is the von Karman constant.

There is a region or gap between the top of the SL and the bottom of the UL where SL similarity theory was not designed to work, and indeed where it has been shown (Santoso and Stull, 1998) to give rather poor results. In this region, one might expect that both SL and ML scales should be important.

To better explain the portion of the boundary layer below the UL, Santoso and Stull (1998) analyzed data from the 1973 Minnesota field experiment (Izumi and Caughey, 1979), and identified a radix layer (RxL) that obeys a similarity scaling different than Monin - Obukhov. The word "radix" means "origin" or "root" in Latin, because the roots of convective thermals are in this layer. The new RxL scaling was found to apply to the whole region between the surface and the bottom of the UL, and thus includes the traditional SL as a subdomain. Typical depths of the RxL are on the order hundreds of meters for wind profiles and tens of meters for temperature profiles.

Based on the definitions above there is superposition of layers; namely, the ML contains the RxL as a subdomain, and the RxL contains the SL as a subdomain). At the top of the RxL, wind speed (M) become tangent to the UL, allowing one to define the top of the RxL as the lowest altitude where $\partial M / \partial z = 0$. Within the RxL, SL scales decrease in importance with increasing altitude, while ML scales increase.

Using data collected in the Minnesota field experiment, Santoso and Stull (1998) proposed similarity equation for wind profiles within and above the RxL. When the dimensionless ratio of wind speed or potential temperature divided by their UL values were plotted against dimensionless ratio of height divided by RxL depth, the data points collapsed quite tightly around the proposed similarity curves. There was also evidence that some of the parameters in these similarity equations were universal.

While these results showed promise for universal similarity profiles in the RxL, there were two drawbacks. First, the success of the theory depended on knowledge of the RxL depth, but this depth was difficult to pinpoint from the observations because of the gradual blending of the wind and potential temperature profiles into the UL. Second, the mechanisms that control the RxL depth had not yet been identified in that first paper. These two drawbacks limited the applicability of RxL theory.

The purpose of this chapter is to improve the data-analysis methodology, and to define new similarity profiles for the RxL that eliminate the drawbacks mentioned above. Buckingham Pi dimensional analysis will be utilized to identify the relevant dimensionless groups of variables, and to help find the parameters that control RxL depth. Convective transport theory (Stull, 1994) will be used to relate surface fluxes to ML scales, and combine these scales with RxL profiles to create new flux-profile relationships.

New parameterization of the RxL depth and improved RxL profile equation for winds are presented. Data from the Minnesota field experiment are used to recalibrate the new parameterization and similarity equation, and data from BLX96 are used to determine whether RxL wind profile depends on surface conditions such as roughness. The results are compared against independent data collected during the Koorin field campaign. A flux-profile relationship is proposed, followed by summary and recommendations.

2. NEW RADIX LAYER THEORY

The first step in any similarity analysis is to hypothesize which variables are relevant to the physics. Because thermal structures exist within the whole ML including the SL, it can be inferred that similarity theory for RxL should depend on both SL and ML parameters. For wind profiles, it was shown in santoso and Stull (1998) that RxL depth, z_{RM}, are the relevant height scale, and that the winds in the UL, $\overline{M}_{UL}$, is the relevant velocity scale. Additional constraints are that the partial derivatives of this mean variable with respect to height is zero at the top of and above the RxL.

2.1. Radix-Layer Depth Equation

Santoso and Stull (1998) showed that the RxL depth for wind, z_{RM}, calculated individually using this method (with zero vertical gradient as the desired constraint) was very sensitive to even small errors in measured data. With such high uncertainties, the attempted parameterization of the RxL depth for winds as a function of SL and ML variables were less successful. To overcome the sensitivity problem, a new approach is taken to parameterize RxL depth as functions of both ML and SL scales, because of the superposition of large buoyantly-driven and small shear-driven eddies in the RxL. The large eddies scale to mixed layer depth, z_i, and Deardorff velocity, w_* (Deardorff, 1970, 1972; Deardorff et al., 1980; Wyngaard et al., 1971; Kaimal et al., 1976; Sorbjan, 1986; Stull, 1988). The small eddies scale to the RxL depth, z_{RM}, and friction velocity, u_*. The small-eddy length scale of RxL depth was chosen because the shear needed to generate shear-driven eddies exists only within the RxL.

Using Buckingham Pi analysis (Stull, 1988) with this set of scales (z_{RM}, z_i, u_*, w_*) yields RxL dimensionless groups of z_{RM}/z_i and u_*/w_*,. The relationship between these groups is not given by Buckingham Pi analysis, and must be found empirically. Such a relationship is

$$z_{RM} = C_M \left(\frac{u_*}{w_*} \right)^{B_M} \cdot z_i \qquad (3)$$

where B_M and C_M are empirical constants. Relationship (1) agrees with the suggestions of Plate (1998) that the base of the UL should be proportional to u_*/w_*. Equation (3) will be tested with Minnesota data.

The parameterization of the RxL depth for winds has a functional form similar to that of the Obukhov length, except that the exponents might be found to differ. It will be shown later that there is a simple relationship between the RxL depth and the Obukhov length.

2.2. Revised RxL Profile Equation

Based on the arguments above, new empirical equation for wind profiles in the RxL ($z \le z_{RM}$) and UL ($z > z_{RM}$) are proposed:

$$\frac{\overline{M}}{\overline{M}_{UL}} = F(z) \qquad (4)$$

where $F(z)$ is a function of the form

$$F(z) = \begin{cases} \left\{ \left(\frac{z}{z_{RM}} \right)^{D_M} \right\}^{A_M} \cdot \exp\left[A_M \left\{ 1 - \left(\frac{z}{z_{RM}} \right)^{D_M} \right\} \right] & for \quad z \le z_{RM} \\ 1 & for \quad z > z_{RM} \end{cases} \qquad (5)$$

and A_M and D_M are empirical profile-curvature parameters. Two shape parameters (A_M, D_M) appear in (5) instead of only one (A) in the old RxL equation (Santoso and Stull, 1998), because the profile shape depends on both meteorological and surface characteristics. The formulation of (5) is designed to allow separation of these two effects, with D_M depending on surface characteristics and A_M on other meteorological characteristics. The net result is that the exponential portion of (5) contributes more than it did in Santoso and Stull (1998), relative to the "power law" portions of that equation.

Substituting (3) into (5) yields a new equation for the wind profile functions:

$$F(z) = \begin{cases} \left\{ \left(z_{*M} \right)^{D_M} \right\}^{A_M} \cdot \exp\left[A_M \left\{ 1 - \left(z_{*M} \right)^{D_M} \right\} \right] & for \quad z \le z_{RM} \\ 1 & for \quad z > z_{RM} \end{cases} \qquad (6)$$

where the dimensionless height is:

$$z_{*M} = \frac{1}{C_M} \cdot \frac{z}{z_i} \cdot \left(\frac{u_*}{w_*} \right)^{-B_M} \qquad (7)$$

As will be shown later, all heights including the RxL depth should be measured from a datum defined as surface elevation plus a displacement distance. That is, over forest canopies and other regions of significant displacement distance z_d, replace all heights z in equations (4) to (7) with $z - z_d$, where z is still measured with respect to the physical surface.

These revised profile equations (4 – 7) identically satisfy the zero-gradient condition at the top of the RxL for any values of the empirical parameters. The resulting mean profiles and vertical gradients in the RxL are continuous, and smoothly merge into the overlying UL. Also, the new profile equation is not a function of RxL depth, thereby eliminating one of the problems of the previous parameterization. As will be shown later, an iterative-graphical procedure can be used to simultaneously solve for B_M, C_M and z_{RM} values that cause field-experiment data to collapse about a common profile curve with minimum scatter.

The equation for the RxL depth (3) and the dimensionless similarity equations for mean profiles (4 – 7) are the basis for the RxL theory for winds as used in the remainder of this paper.

3. EMPIRICAL PARAMETERS

The parameters in any similarity theory must be determined empirically. As discussed in the earlier paper, calibration of RxL parameters requires statistically robust wind data that are consistent and contiguous from near the surface through the interior of the ML. One cannot use data that have profile gaps and mismatches, such

as are typical of field experiments where instantaneous rawinsonde observations in the middle of the ML are combined with time-averaged observations from instrumented towers in the SL.

Data from three field experiments have been found to satisfy the requirements. Data from one of the experiment sites, Minnesota, is used in this section to find (i.e., calibrate) the RxL empirical parameters of (3 – 7). In later sections, the terrain roughness dependence of the parameters is determined using BLX96 field data. Finally, the results are compared with independent data from the Koorin field campaign.

3.1. Methodology — Separation of Parameters

Parameters A_M and D_M appear only in the profile shape equation (6), while parameters B_M and C_M appear in the dimensionless height z_{*M} definition (7). This separation of parameters allows one to empirically solve for the best-fit values of B_M and C_M first, independent of the as-yet-unknown values of A_M and D_M. Such an approach overcomes the sensitivity problem in calculating the RxL depths that plagued the original RxL paper.

To get B_M and C_M for winds, first estimates the values of wind speed in the UL. Then, plot the observed data in the form of dimensionless wind $\overline{M}(z) / \overline{M}_{UL}$ against dimensionless height z_{*M}. The result will be a cloud of points clustered along a vertical profile. An iterative approach is then used to vary parameters B_M and C_M until the cloud of points exhibits the tightest packing.

The end result is shown in Fig. 1 for all 11 runs of the Minnesota experiment (ignore the solid line for now). The figure also includes plots in semi-log form to show more detail near the surface. These Minnesota data collapse very tightly into a similarity curve for this new RxL approach, much like they did for the old approach shown. Hence, the new RxL approach in this paper is still an effective similarity theory. The resulting best fit parameter values are C_M = 1/2 and B_M = 3/4. Knowing constants B_M and C_M, the RxL depth for wind can be calculated using (3) for each Minnesota run. Once the RxL depth is known, then those data points above the RxL depth can be averaged to give the mean wind speed in the UL, $\overline{M}_{UL}$, for each run.

If necessary, these revised values of UL wind can be used to re-estimate B_M and C_M as described in the previous two paragraphs.

To get A_M and D_M, a non-linear regression is applied to minimize the sum of squared errors between the regression equation (4, 6, and 7) and the data, where both the RxL and UL are taken together when calculating squared errors. In Fig. 1, this corresponds to finding the solid line that best fits the cloud of data points. Using all 11 Minnesota runs, one finds that A_M = 1/4 and D_M = 1/2.

Fig. 2 compares the old vs. new values of

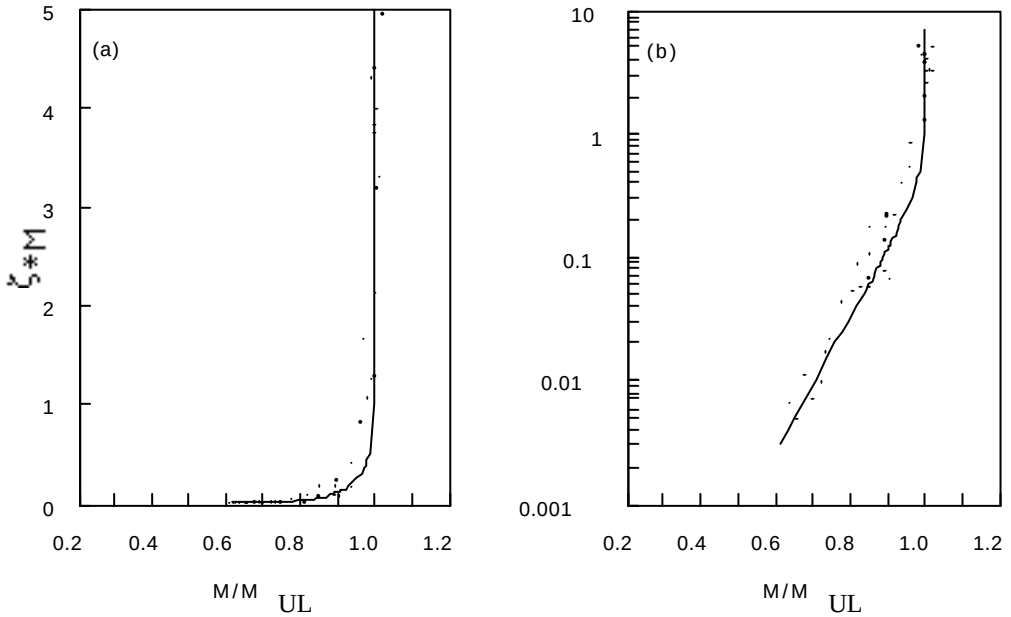

Fig. 1. Dimensionless wind speed profiles for the Minnesota data, plotted in form using RxL similarity theory uses (a) linear axes to focus on the UL and top of the RxL, and (b) semilog axes to focus on the middle and bottom of the RxL

RxL depths for winds. There is similar scatter for both variables, confirming that RxL depth should not be used as a similarity variable, and that RxL depth is difficult to determine from observational data because it is the height where the profile gradually blends into the UL. This is further justification for using (7) to define a dimensionless height in the RxL, rather than using z / z_{RM} .

The Minnesota field experiment data do not allow one to test whether the RxL profiles are directly a function of surface roughness length, because the experiment was conducted over just one site with fixed roughness. Roughness effects will be examined later using data from the BLX96 experiment, because it was conducted over three sites with different land surface characteristics.

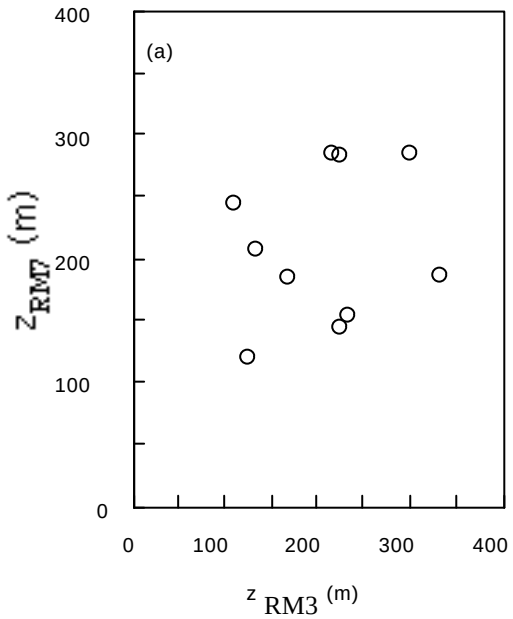

Fig. 2. Comparison of the RxL depths for winds found from the individual best fit values to the observations and from the parameterization for the Minnesota field experiment.

3.2. Relationship between the RxL Depth and the Obukhov Length

Because the Obukhov length and the RxL depth are both boundary-layer length scales, it is instructive to compare them. Combining the definition for the Obukhov length (2) with the definitions for Deardorff velocity (1) allows one to rewrite the Obukhov length as:

$$L = -\frac{1}{k} \cdot \left(\frac{u_*}{w_*} \right)^3 \cdot z_i \qquad (8)$$

which has some similarities to (3). When the RxL depth (3) is used with the best-fit parameters found above, one can relate the RxL depth and the Obukhov length for the statically-unstable boundary layer

$$z_{RM} = C_M \left\{ k \cdot (-L) \cdot z_i^{\,3} \right\}^{1/4} \qquad (9)$$

The Obukhov length is more strongly dependent on the ratio of u_* / w_* than the RxL depth. Similar to the Obukhov length, the RxL depths are indirectly related to surface roughness length z_o via the friction velocity u_*.

4. TERRAIN ROUGHNESS DEPENDENCE

To determine whether surface conditions such as aerodynamic roughness z_o or topography influence the wind RxL profiles and depths, data from BLX96 are analyzed next. Components of the BLX96 experiment were designed specifically to examine this issue.

4.1. Data Analysis Procedure

As was discussed in Berg et al. (1997), Stull et al. (1997), Santoso (2000), a vertical zigzag flight pattern was flown over a 70 km horizontal distance to provide vertical profiles of horizontal mean wind, temperature and humidity between altitudes of about 10 m and 700 m above ground level (AGL). This spans the SL, the RxL and the bottom of the UL. To get vertical profiles, the data are sorted by altitude into non-overlapping bins of 2 m vertical depth. The average value within each bin is assigned to a height at the bin center, and is based on an average of at least 50 observations per plotted point. As was shown in Santoso (2000), the resulting wind data show some scatter, but the large number of data points helps improve the statistical robustness of the sample.

To find the ML depth z_i, higher ascent/descent soundings were flown at the beginning, middle and end of each of the four-hour flights. These were interpolated to the midtimes of the zigzag flights to account for the ML nonstationarity. Deardorff velocity, heat flux, buoyancy flux and were calculated iteratively using (1), $\overline{w'q'}_s = C_{*H} \cdot w_* \cdot \Delta\overline{q} + \overline{w'q'}_o$ [see equation (6) and the constants for BLX96 in Santoso (2001)] and $\overline{w'q_v'}_s \approx \overline{w'q'}_s \cdot \left(1 + 0.61 \cdot \overline{r}\right) + 0.61 \cdot \overline{q} \cdot \overline{w'r'}_s$, where r is mixing ratio and $\overline{w'r'}_s$ is surface kinematic moisture flux. Momentum flux magnitude (equal to the square of the friction velocity u_*) was estimated using $u_* = C_{*D} \cdot w_* \cdot \overline{M}_{UL}$ [see equation (1) and the constants for BLX96 in Santoso (2000)].

4.2. RxL Parameters for BLX96

The depth of the RxL for wind speed is estimated using (3) for each leg. Because these RxL depths define the location of the bottom of the UL, the mean wind speed in the UL are determined next. Finally, these are all used to give dimensionless profiles of mean wind speed: $\overline{M}(z)/\overline{M}_{UL}$ vs. z_{*_M}. Wind data from the Meeker July 28 leg AA were excluded from the Meeker plot, because wind was so slow (about 1.5 m/s) that $\overline{M}_{UL}$ was of the same order as w_*, resulting in excessive sampling noise.

The dimensionless profiles for the remaining 18 cases are plotted in Figs. 2 – 4 for the Lamont, Meeker and Winfield sites. The height parameters in these plots have been corrected by the displacement height z_d due to pasture, cropland and forest. As recommended by Garratt (1978), the displacement height z_d is taken as 64% of the estimated roughness-element height average. The displacement heights for individual vegetation types (trees, pasture, etc.) were weighted by the relative coverage of those types under each flight path footprint to give flight-leg averaged values. The resulting displacement heights for Lamont, Meeker and Winfield are 0.3 m, 2.7 m and 1.8 m, respectively.

Next, the parameters B_M and C_M are calculated to determine if they are significantly different from those for Minnesota. Within the scatter of these BLX96 data sets, there is no significant difference, suggesting that B_M and C_M might be universal constants rather than parameters.

Because parameters B_M and C_M did not vary from those of Minnesota, one might ask if parameters A_M and D_M are also constant. The RxL wind profile equations using the Minnesota parameter values of A_M and D_M are plotted in Figs. 3 – 5 as the dashed lines, along with the BLX96 data points. The solid lines in these figures represent the RxL profile using parameters that are the best fit for the BLX96 data using non-linear regression as was done for the Minnesota data.

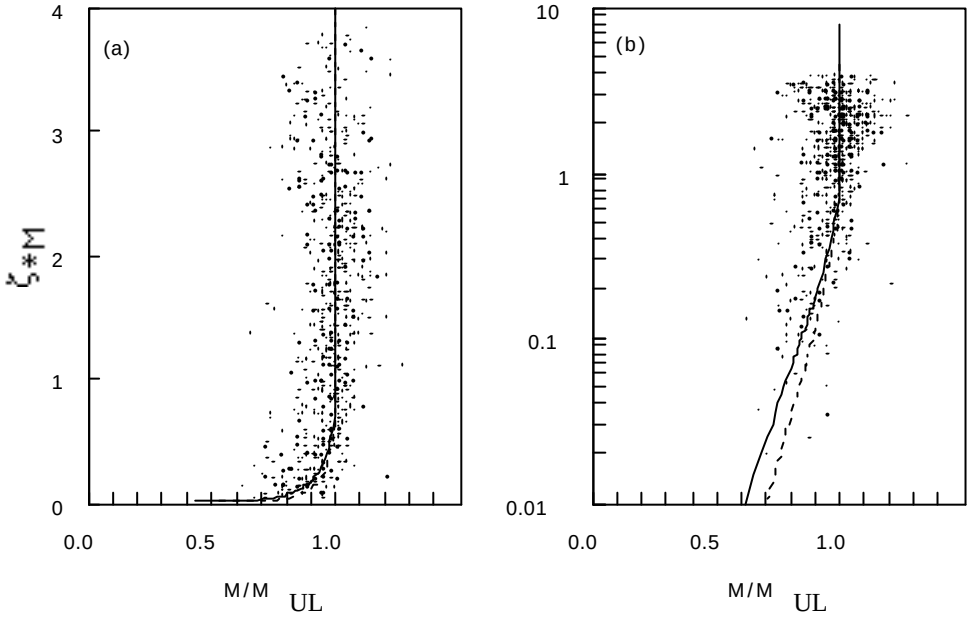

Fig. 3. Vertical profiles of dimensionless wind speed for the BLX96-Lamont site. Data points are from all 7 flights at the Lamont site. The solid line is the RxL profile using the best nonlinear regression parameters for this data, while the dashed line is the RxL profile using parameters from the Minnesota field experiment. Again, (a) is in linear-linear coordinates, while (b) is vertically logarithmic to show more detail in the bottom of the RxL.

However, for winds, the Minnesota parameter values do not provide the best fit to the data for all sites, as exhibited by the difference between dashed and solid lines. Further analysis revealed that these site-to-site profile differences of wind could not be explained by parameter A_M. Namely, the best fit A_M value for BLX96 was negligibly different from the best fit Minnesota value, and will be considered a constant here.

This leaves D_M as the key parameter to describe terrain characteristics. When holding A_M constant, the non-linear regression best fit values of D_M for BLX96 are D_M = (0.62, 0.73, 0.89) for (Lamont, Meeker, Winfield), which are the solid lines plotted in Figs. 3 – 5. When these values of D_M were plotted against aerodynamic roughness length z_o, no significant correlation was found (correlation coefficient = 0.24). When

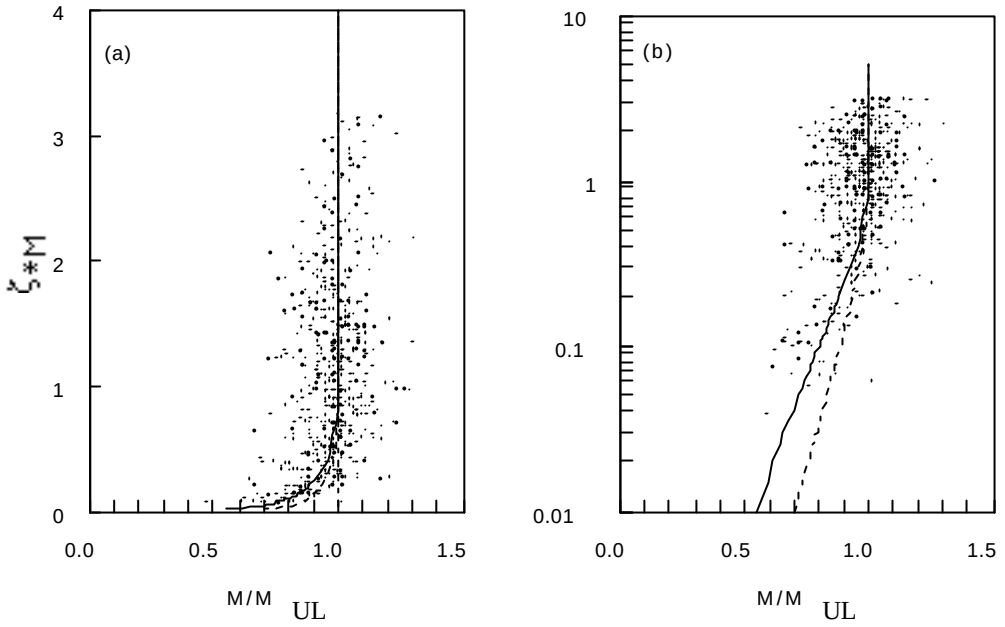

Fig. 4. Same as Fig. 3, but for 6 flights at BLX96-Meeker site (excluding wind data from the 28 July 96 leg AA flight).

plotted against the displacement height z_d, again no significant correlation was found. Based on this limited data set, it is concluded that neither aerodynamic roughness nor displacement height can explain the site-to-site variation of profile curvature (i.e., of parameter D_M). So there must be some other characteristic that causes D_M to vary from site to site for this BLX96 data set.

Next the larger-scale topographic variability was investigated to try to explain the differences between the sites. Fig. 6 shows plots of surface elevations above MSL, under the Lamont, Meeker and Winfield flight tracks, which were flown approximately east-west. By eye, the Lamont surface topography (Fig. 6a) appears relatively smooth and flat, and has the smallest D_M. Winfield (Fig. 6c) has the roughest topography, and has the largest D_M. These plots suggest that resolvable topographic characteristics might have caused the variation of D_M.

To better quantify such a relationship, the discrete variance (energy) spectrum of the surface topography for each site is analyzed. From horizontal low-level aircraft flights, measurements of aircraft pressure altitudes and radar altitudes AGL sampled at 1 Hz, are used to estimate

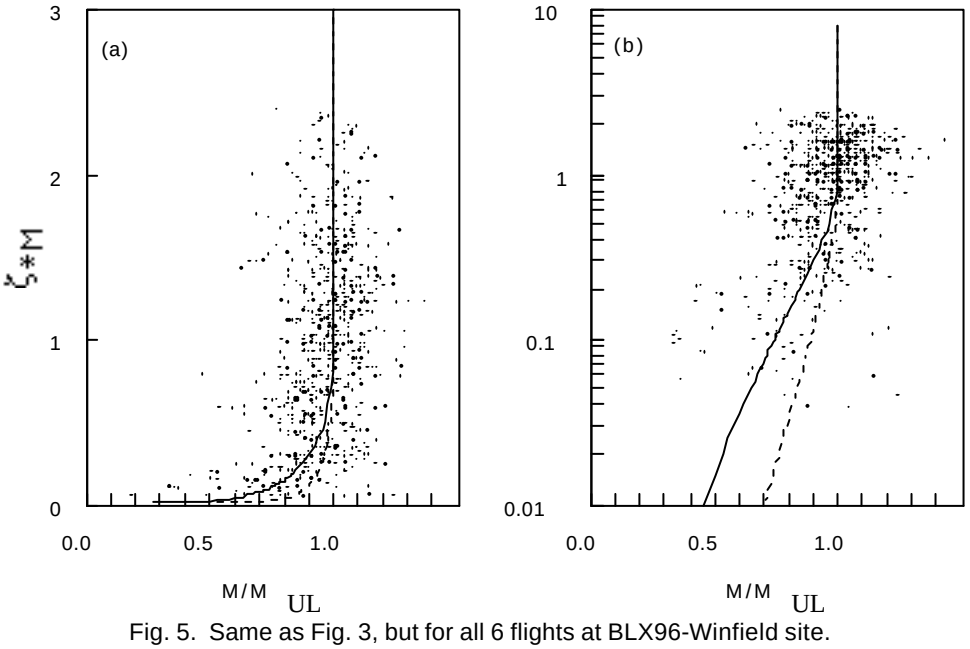

Fig. 5. Same as Fig. 3, but for all 6 flights at BLX96-Winfield site.

surface elevations above MSL under the aircraft. Using a Fourier transform, these 1 Hz surface elevations under the Lamont, Meeker and Winfield tracks are converted from frequency space (after the mean and trend were removed) to wavenumber space, to get the total spectral energy density at each site.

To allow better comparison of the discrete variance (energy) spectrum between the sites, the time series from all sites is truncated to be the same length as the shortest time series (still corresponding to roughly 70 km horizontal flight distance) for each flight track. Many low-level flights were flown over each site following virtually the same track based on GPS navigation. Results show that the total spectral energy density (e.g., total variance) from flight to flight over the same site varies by about 6% of the total variance, supporting the assertion that the flights were virtually over the same track at any one site. The standard deviations of elevations for the Lamont, Meeker and Winfield tracks were s_z = 12.9 m, 16.8 m, and 30.2 m, respectively. These are plotted as the (o) data points in Fig. 7. Also in Fig. 7 is the corresponding data point (x) from the Minnesota field experiment. This experiment was over a single location rather than being along a flight track, and no terrain spectra were provided in the Minnesota data book. Therefore, a spectral analysis of current digital elevation data (from the US Geological Survey website: 1 m contour accuracy, 30 second interval distance) was performed for the Minnesota field site, assuming that topography has not changed significantly since 1973 (in contrast to aerodynamic roughness which usually does change as vegetation and snow cover varies). The resulting standard deviation of elevation s_z = 12.2 m. Even though the crop characteristics and recent plowing of neighboring farm fields at Minnesota were similar to those at Lamont (and therefore might be expected to have nearly equal values of

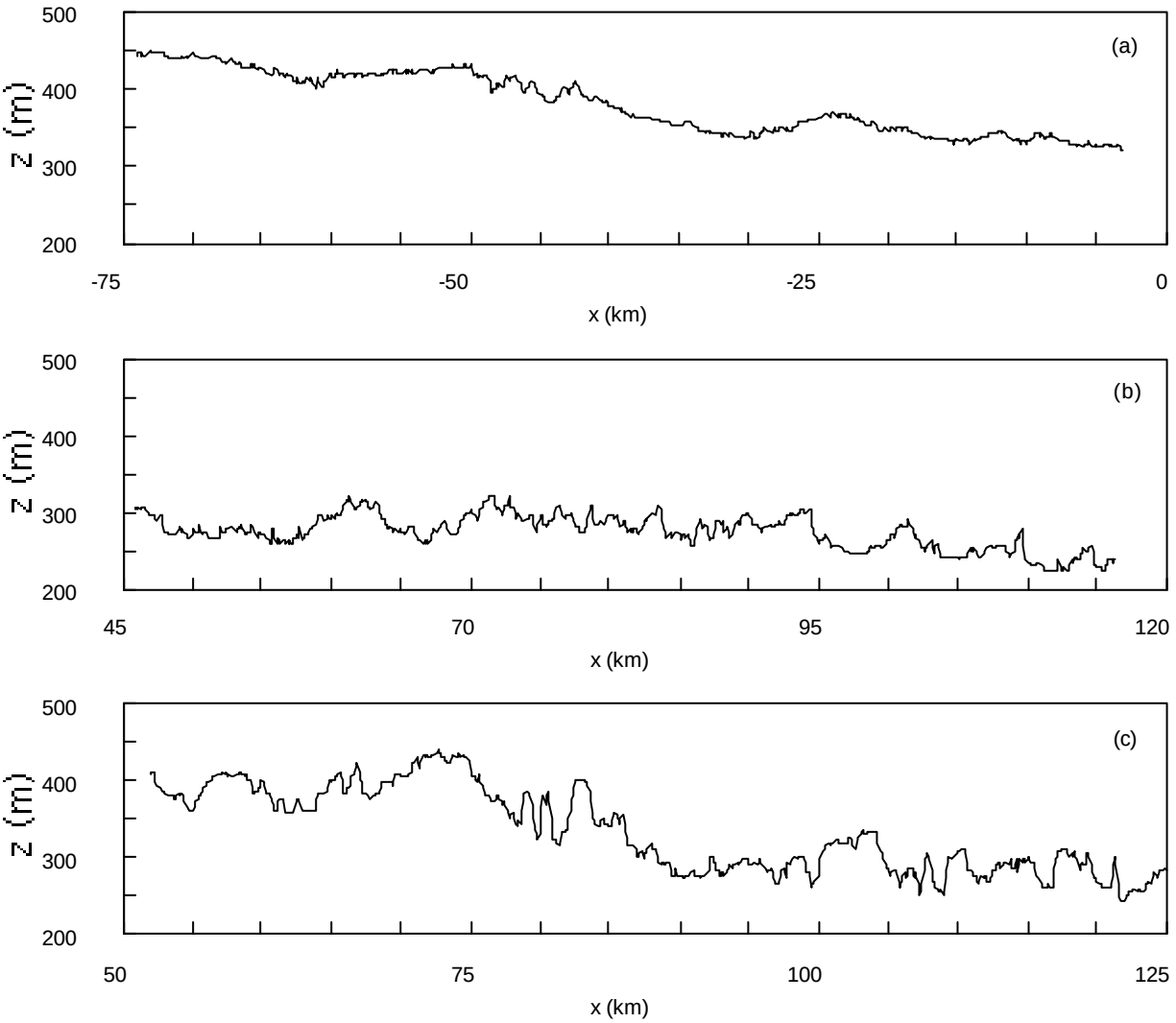

Fig. 6. Terrain elevation above MSL under the BLX96 flight paths at (a) Lamont, (b) Meeker, and (c) Winfield.

aerodynamic roughness length), the Minnesota site has slightly smoother resolvable surface topography. Thus, the Minnesota site has smaller standard deviation of elevation than any of the BLX96 sites, and corresponds with the smallest best-fit value of D_M .

The variations of parameter D_M were found to be highly correlated (correlation coefficient = 0.92) to the standard deviation topography elevation σ_z:

$$D_M = a + b \cdot \sigma_z \qquad (9)$$

where a = 0.35 is dimensionless and b = 0.018 m^{-1} . This relation is shown in Fig. 7 as the straight line. The conclusion is that rougher terrain-elevation variations cause greater curvature in the wind-speed profile, as indicated by large values of D_M .

Unlike the ML transport coefficient C_{*D} for momentum fluxes that was found to be dependent on surface roughness length z_o (Santoso, 2000), the curvature parameter D_M for RxL wind profiles is dependent on standard deviation of elevation σ_z. These different dependencies are probably due to differences in their measurement heights. The momentum fluxes are measured close to the surface, therefore, local surface elements and obstacles that create the aerodynamic roughness have more influence on these near-surface (z = tens of meters) measurements. For RxL wind profiles that span heights of order hundreds of meters, the local surface elements or obstacles are felt only by the near-surface part of the RxL wind profiles. The higher part of the wind profiles are not influenced by local surface elements, but are more likely influenced by much larger footprint area (e.g., surface topography). Thus, it is not surprising that the RxL wind profiles are dependent on standard deviation of surface topography via the curvature parameter D_M .

An obvious question is why the RxL wind profile apparently depends on terrain characteristics. One explanation is that the wind profile has surface skin values that are always zero, regardless of wind speed in the UL. Thus, the magnitude of wind shear and of surface stress must always reflect the frictional drag at the surface. A similar explanation also applies to CTT (Stull, 1994), which was also found to have momentum flux parameters that do depend on roughness (see Santoso, 2000).

5. COMPARISON WITH KOORIN DATA

From Fig. 7 in the previous section, data from both Minnesota and BLX96 were used to find a relationship between the parameter D_M and the standard deviation of resolvable terrain roughness σ_z. The other RxL wind profile parameter was suggested to be constant, based on those same field experiments. These parameters in the RxL wind profile equation will now be compared against independent data from the Koorin field experiment.

The Koorin experiment was conducted in Northern Australia at a site with with small hills that ranged from 40 to 60 m in height [see Figs. 1.1 and 5.3 in Clarke and Brook (1979)]. Within 50 km radius from the observation site the surface topography was quite flat. Vegetation coverage in that region consisted of a forest of well-spaced and uniformly distributed eucalyptus and acacia trees of height 5 to 10 m, with sparse grass beneath. The roughness length at Koorin was z_o = 0.4 m and the displacement distance was z_d = 5.1 m. Based on the resolvable terrain roughness (calculated from a 1:100,000 scale topographic map, with contour interval of 20 m), the standard deviation of terrain elevation is approximately σ_z = 13.0 m.

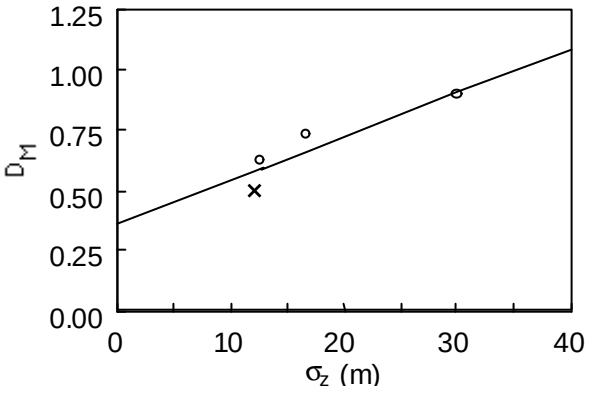

Fig. 7. Variation of the wind-profile shape parameter D_M with respect to standard deviation of terrain elevation σ_z for BLX96 (o) and Minnesota (x), and the corresponding linear regression (solid line).

Measurements were taken at Koorin during the winter (15 July – 13 August 1974). Vertical fluxes of momentum, heat and moisture were determined using the eddy correlation technique. Mean wind speeds were measured at heights of 11.55, 15.65, 22.15, 32.15 and 48.65 m, and temperature sensors were mounted 0.63 m lower. All were above canopy-top heights. There were 118 experimental runs made during 30 days of convective conditions, giving a total of nearly 600 wind-profile data points. In addition to the tower measurements, there were less-frequent radiosonde soundings to greater height.

Observation periods for the mean winds, heat, moisture and momentum fluxes were identical, but the averaging time for mean wind

speed was an hour while for the fluxes was a half an hour. These averaging times are sufficiently long to give robust statistics and smooth wind profiles. ML depths z_i were estimated from soundings, and were used in the calculation of Deardorff velocity (1). RxL depths are then estimated using (3).

Unfortunately the radiosonde soundings cannot be used to give UL characteristics, because the soundings suffer from the lack of statistica robustness described earlier (the difficulty of merging instantaneous soundings with time-average SL winds). Instead, $\overline{M}_{UL}$ must be inferred from RxL wind profiles. Equations (4 – 7) can be used to solve for $\overline{M}_{UL}$ values for each profile. Because the data are used to help determine one of the parameters ($\overline{M}_{UL}$) in each profile equation, it means that one cannot independently test the quality of the proposed RxL profile equations and parameters. This is a very unfortunate limitation of the Koorin data set. However, the available data do allow one to compare the shape or curvature of the profile equations (4 – 7) to the shape of the plotted data, because these shapes are not affected by the value of wind speed in the UL..

The RxL wind parameter values are taken as constants as previously discussed: A_M = 1/4,, B_M = 3/4, and C_M = 1/2, except that D_M = 0.59 was found from Fig. 7 (or calculated from Eq. 9) based on the resolvable terrain roughness of σ_z = 13.0 m at Koorin. The resulting RxL profile curves for wind are plotted in Fig. 8a, and fit the data quite well.

Given the limitations of the comparison described above, at best one can conclude from the Koorin field program that the shape of the profile equations agrees very well with the shape of the data, and that the data collapse tightly into a single similarity curve after properly accounting for displacement distance.

6. FLUX-PROFILE RELATIONSHIP

The RxL wind profile equation is a function of the difference of mean wind values between the surface skin and the UL. CTT relates surface momentum fluxes to the difference of mean wind values between the surface skin and the UL. By combining these two theories, one can relate the fluxes to the profiles, resulting in new flux-profile relationships for wind in the RxL.

Substituting CTT equation for momentum [see Eq. (1) in Santoso (2000)] to wind profile equations (5) and (6) yields a flux-profile relationship for mean wind speed in the RxL:

$$\overline{M}(z) = \frac{{u_*}^2}{C_{*D} \cdot w_*} \cdot F\left(z - z_d, z_i, u_*, w_*\right) \quad (10)$$

The flux-profile relationship for wind speed (10) is dependent on a wide-range of scales of terrain roughness. First the ML transport coefficient for momentum flux C_{*D} depends on small-scale roughness elements as affect the aerodynamic roughness length z_o. Second, parameter D_M depends on resolvable-scale topographic variations as affect the standard

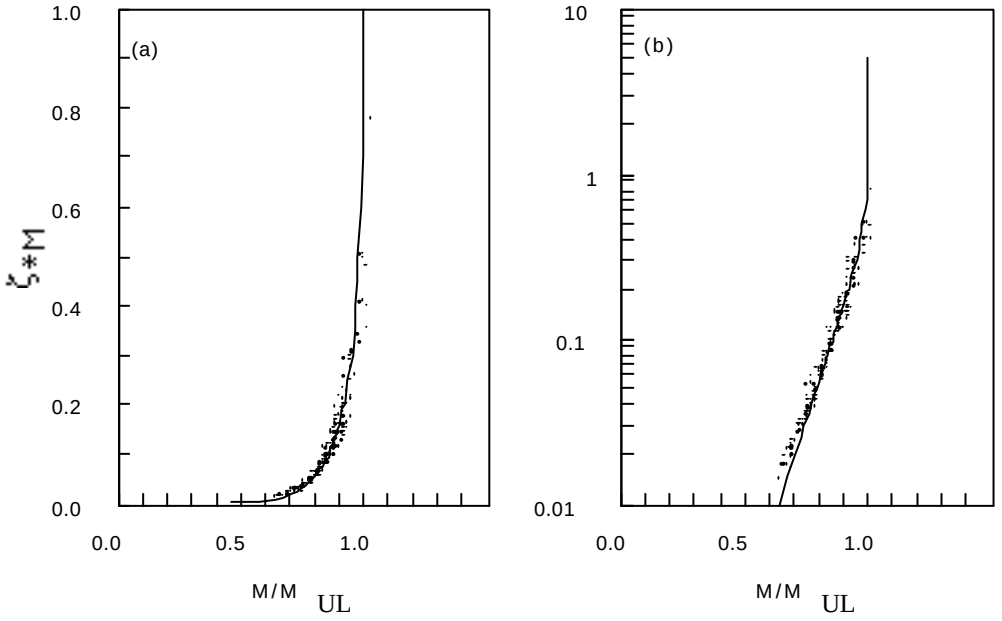

Fig. 8. Same as Fig. 3, but for Koorin site. for wind speed is using D_M = 0.59 (based on Eq. 9), and applying the aerodynamic displacement distance.

deviation of terrain elevation s_z. Such dependence over the wide range of scales should be expected because the RxL profile equations were designed and calibrated as the average over a heterogeneous region (e.g., by using 72 km flight legs in BLX96), rather than being for one column over a single land use.

Equation (10) is easy to use to diagnose wind profiles given measurements of surface heat flux, momentum flux, and ML depth. However, it is more difficult to go in the other direction to get the fluxes from the profiles. The reason is that the profile function F depends on the surface fluxes hidden in u_* and w_*. Nonetheless, there are many nonlinear regression packages available (e.g., Press et al., 1992) that can easily solve (10) for the fluxes, given observations of the mean wind profiles in the RxL. Also, the fluxes in this equation are related to the shape of the profiles in the RxL and are not a function of surface skin or UL properties, allowing the fluxes to be estimated using less expensive anemometers and thermometers at various heights along a mast or tower.

Similar difficulties are encountered when obtaining the fluxes from classical Businger-Dyer flux-profile relationships for the unstable surface layer, which are of the form (see Paulson, 1970; Stull, 1988):

$$\overline{M} = \frac{u_*}{k}\cdot\left[\ln\left(\frac{z}{z_o}\right) - 2\ln\left(\frac{1+x}{2}\right) - \ln\left(\frac{1-x^2}{2}\right) + 2\tan^{-1}(x) - \frac{p}{2}\right] \quad (11)$$

where $x = (1-15z/L)^{-1/4}$, assuming z_o/L is negligible. Again the fluxes are hidden in each term containing the Obukhov length L.

7. SUMMARY AND RECOMMENDATIONS

The depth of the RxL is given by (3), and depends both on mixed-layer characteristics such as ML depth, and on surface characteristics such as heat and momentum fluxes. These new depth equations eliminate the uncertainty in RxL depth that were discussed in a previous paper (Santoso and Stull, 1998).

Similarity shapes of RxL wind profiles are given by (4 – 7). These equations are designed to give zero wind speed at the ground (or at the displacement height for forest canopies), and to become tangent to the UL wind speed at the top of the RxL. These apply only during convective conditions, when thermals are the more dominant turbulence process. They have been calibrated to work for mesoscale (order of 50 km) regions over heterogeneous surfaces. These equations are not applicable in the blending layer and the roughness sublayer, in the immediate vicinity of the individual roughness elements.

The RxL depth parameterization includes two parameters: B_M and C_M. The profile equations include two more parameters A_M and D_M. Based on the five field sites examined here (Minnesota, BLX96-Lamont, BLX96-Meeker, BLX96-Winfield, and Koorin), all but one of the parameters are constant, suggesting that they might be universal. Only the D_M parameter for wind depends on surface terrain characteristics, and surprisingly does not depend on traditional aerodynamic roughness length.

The equation for RxL depth is similar to the equation for Obukhov length, which is a function of shear forces and buoyant forces. As shown in (8) there is a simple relationship between RxL depth and Obukhov length, although the RxL depth also includes a stronger dependence on ML depth. The RxL depth varies from day to day, analogous to the variability of Obukhov length, because both depend on varying external forcings.

A flux-profile equation for winds in the convective RxL has been suggested in (10), which extends over a greater depth that traditional surface-layer Monin-Obukhov flux-profile relationship. The dimensionless form of this flux-profile relationship is in terms of the mean profiles of wind, rather than of their gradients. As was discussed in a

Finally, the data from Minnesota and Koorin show much less scatter than the data from BLX96. There are two reasons. One, the Minnesota and Koorin data are measured over single points on the earth's surface having relatively homogeneous surroundings, compared to the BLX96 data which was measured by aircraft over a 72 km distance having surface heterogeneity. Second, the long time averages from multiple sensors at different heights during Minnesota and Koorin provided more robust statistics than the sequentially-sampled heights by aircraft flying ascent-descent zig-zag patterns during BLX96. For further tests of the equation, it would be very appropriate for other investigators to analyze meteorological data from very tall instrumented towers, which would likely produce very statistically robust data.

Potential applications for wind speed diagnoses using the RxL equation includes air-pollutant transport, wind loading on bridges and other tall structures, and calculating power output from wind turbines. The wind profile equation could be used in forecast models to estimate vertically-unresolved effects associated with relative coarse vertical grid spacing, but only during convective conditions.

REFERENCES

Berg, L. K., R. B. Stull, E. Santoso, J. P. Hacker, 1997: *Boundary Layer Experiment - 1996 (BLX96) Airborne Scientist Flight Log*. Boundary Layer Research Team Technical Note BLRT- 97-1. 116 pp.

Businger, J. A., J. C. Wyngaard, Y. Izumi and E. F. Bradley, 1971: Flux-profile relationships in the atmospheric surface layer. *J. Atmos. Sci*., **28**, 181 -189.

Clarke, R. H. and R. R. Brook, 1979: *The Koorin Expedition, Atmospheric Boundary Layer Data over Tropical Savannah Land*. Bureau of Meteorology, Australian Government Publishing Service, Canberra. ISBN-0-642-01484-1. 359 pp.

Deardorff, J. W., 1970: Convective velocity and temperature scales for the unstable planetary boundary layer and for Rayleigh convection. *J. Atmos. Sci*., **27**, 1211 - 1213.

Deardorff, J. W., 1972: Numerical investigation of neutral and unstable planetary boundary layers. *J. Atmos. Sci*., **29**, 91 - 115.

Deardorff, J. W., G. E. Willis and B. H. Stockton, 1980: Laboratory studies of the entrainment zone of a convectively mixed layer. *J. Fluid Mech.*, **100**, part 1, 41 - 64.

Dyer, J. A., 1974: A review of flux-profile relationship. *Bound.-Layer Meteor.*, **7**, 363 - 372.

Izumi, Y. and J. S. Caughey, 1976: *Minnesota 1973 Atmospheric Boundary Layer Experiment Data Report*. AFCRL-TR-76-0038. Massachussets. 28 pp.

Garratt, J. R., 1978: Flux profile relationships above tall vegetation. *Quart. J. Roy. Meteor. Soc.*, **104**, 199 - 212.

Kaimal, J. C., J. C. Wyngaard, D. A. Haugen, O. R. Cote and Y. Izumi, 1976: Turbulence structure in the convective boundary layer. *J. Atmos. Sci*., **33**, 2152 - 2169.

Paulson, C. A., 1970: The mathematical representation of wind speed and temperature profiles in the unstable atmospheric surface layer. *J. Appl. Meteor.*, **9**, 857 - 861.

Plate, E. J., 1998: The convective boundary layer: A historical introduction. In *Buoyant Convection in Geophysical Flows.*(Ed. E. J. Plate, E. E. Fedorovich, D. X. Viegas and J. C. Wyngaard). Kluwer academic Publishers, Dordrecht, The Netherlands, 1 - 22.

Press, W. H., B. P. Flannery, S. A. Teukolsky and W. T. Vetterling, 1992: *Numerical Recipes in FORTRAN: The Art of Scientific Computing*, Second Ed., Cambridge University Press 963 pp.

Santoso, E., 2000: Parameterization of surface momentum flux during convective conditions. *J. Sains & Tekn. Mod. Cuaca*, **1**, 33 – 44.

Santoso, E., 2001: Evidence of counter-difference surface heat fluxes and its hypotheses. *J. Sains & Tekn. Mod. Cuaca*, **2**, (in press).

Santoso, E. and R. B. Stull, 1998: Wind and temperature profiles in the radix layer, the bottom fifth of the convective boundary layer. *J. Appl. Meteor.*, **37**, 545 - 558.

Sorbjan, Z., 1986: On similarity in the atmospheric boundary layer. *Bound.-Layer Meteor.*, **34**, 377 - 397.

Sorbjan, Z., 1999: Similarity of scalar fields in the convective boundary layer. *J. Atmos. Sci*. (in press).

Stull, R. B., 1988: *An Introduction to Boundary Layer Meteorology*. Kluwer Academic Publishers, Dordrecht, The Netherlands. 666 pp.

Stull, R. B., 1991: Static stability — an update. *Bull. Amer. Meteor. Soc*., **72**, 1521 - 1529.

Stull, R. B., 1994: A convective transport theory for surface fluxes. *J. Atmos. Sci*., **51**, 3 - 22.

Stull, R. B., 1997: Reply (to comments on "A convective transport theory for surface fluxes"). *J. Atmos. Sci*., **54**, 579.

Stull, R. B., E. Santoso, L. Berg and J. Hacker, 1997: Boundary layer experiment - 1996 (BLX96). *Bull. Amer. Meteor. Soc.*, **78**, 1149 - 1158.

Wyngaard, J. C., O. R. Cote and Y. Izumi, 1971: Local free convection, similarity, and the budget of shear stress and heat flux. *J. Atmos. Sci.*, **28**, 1171 - 1182.

DATA PENULIS

Edi Santoso, lahir di Jakarta, 12 Maret 1960. Menyelesaikan S1 di Jurusan Geofisika & Meteorologi, ITB (1985). Menyelesaikan S2 bidang Atmospheric Sciences, di University of Wisconsin – Madison, USA (1993). Menyelesaikan S3 bidang Atmospheric Science, di University of British Columbia, Vancouver, Canada (1999). Bekerja di UPT Hujan Buatan BPP Teknologi sejak 1986. Sebagai Reseach Assistant di University of Wisconsin – Madison (1994 – 1995) dan di University of British Columbia (1996 – 1999). Sebagai Teaching Assistant di University of British Columbia (1998 – 1999).